Optica Applicata, Vol. XXXV, No. 4, 2005

Optical pumping of an infrared-to-visible upconversion fiber laser

FRANCISZEK KACZMAREK[1*], JERZY KAROLCZAK[1, 2]

[1]Quantum Electronics Laboratory, Institute of Physics, Adam Mickiewicz University, Umultowska 85, 61-614 Poznań, Poland

[2]Center for Ultrafast Laser Spectroscopy, Adam Mickiewicz University, Umultowska 85, 61-614 Poznań, Poland

Corresponding author: F. Kaczmarek, efka@amu.edu.pl

In the previous article (see *Optica Applicata* **31**(2), 2001, pp. 373–6) on laser diode pumping of an infrared-to-visible upconversion fiber laser emitting at 544 nm, special attention was paid to the role of focusing of the incident pumping power. This paper discusses the role of the wavelength dependence of the pumping beam, in particular, the appearance of undesired side fluorescences at 660 and 850 nm, and also the distribution of the pumping power along the fiber length.

Keywords: infrared-to-visible upconversion fiber lasers.

1. Introduction

The infrared-to-visible upconversion fiber laser emitting at 544 nm (erbium-doped ZBLAN fiber) is usually pumped at 970 or 800 nm, applying laser diodes or tunable Ti-sapphire laser. We have used both pumping sources. Pumping at 800 nm generates quite a strong undesired 850 nm fluorescence. It decreases to zero, when the pumping wavelength increases above the 807 nm level [2]. Applying a laser diode pumping at about 807 nm, we have studied the power distribution along the fiber length, and using another laser diode emitting at 970 nm, the appearance of the undesired side fluorescences at 660 and 850 nm. Using laser diodes one has to take into account also the wavelength dependence upon its driving current.

2. Experimental

2.1. Laser diode emission as a function of the driving current

Thermoelectric cooling (TEC) of a laser diode is a standard procedure, however, it does not ensure the stability of the wavelength emitted. The point is that high driving

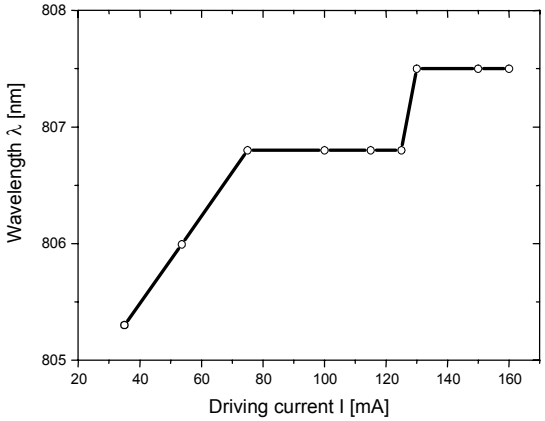

Fig. 1. Emitting wavelengths as a function of the driving current measured for the SDL-5422 single mode laser diode.

current heats the emitter locally and the TEC plate is unable to decrease the temperature to the initially adjusted point. In a standard laser diode (in our case it was a SDL 5422 type), the $d\lambda/dT$ shift amounts to 0.3 nm/deg.

We have measured the wavelength emitted as a function of the driving current, with the TEC cooler fixed at 5°C. There are two wavelength jumps clearly seen in Fig. 1. The jumps are very specific for a determined diode and cannot be generalized. Analyzing the fluorescence or laser emission of a medium pumped with a laser diode as a function of the driving current, one has to take into account these wavelength jumps, and realated changes in the incident power absorbed.

2.2. Display of the pumping power along the fiber length

In a standard optical cavity of a fiber laser, the input mirror is fully transparent for the pumping beam, and the output one should totally reflect the nonabsorbed pumping power back to the resonator. As an example, we have measured first the absorption coefficient α for the ZBLAN:Er^{3+} (1000 ppm) optical fiber at 807 nm (NA = 0.28, core diameter 1.8 μm), to be 0.004 cm^{-1}. Assuming an exponential law, we have plotted the I/I_0 ratio (for the forward direction), and the I'/I'_0 ratio (for the reflected beam), as a function of the position along the fiber (Fig. 2). The fiber was 173 cm in length. The effective pumping power ratio at any point of the fiber is simply $I/I_0 + I'/I'_0$ ($I'_0 = I_0/2$). As a matter of fact, the influence of the reflected power on the intensity of the green fluorescence is clearly seen, when the fiber terminal is being butt coupled to the output mirror.

Contrary to a rather homogenous distribution of the pumping power in bulk laser active media, in case of optical fiber lasers, the pumping power decreases exponentially along the fiber length. In this way, the threshold for laser emission may appear in the first section of the fiber and the rest of it can even absorb the laser beam instead

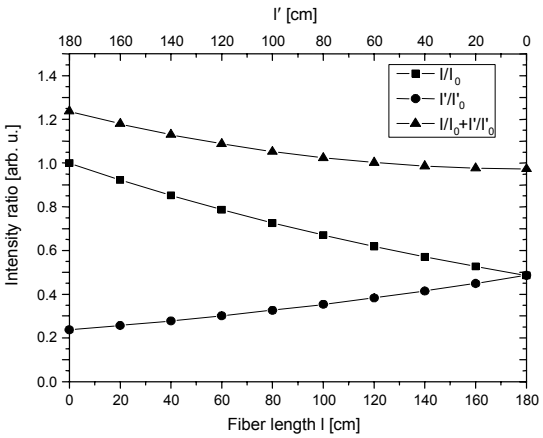

Fig. 2. Distribution of the pumping power along the fiber length within the optical resonator; ■ – forward direction (I/I_0), ● – backward direction (I'/I'_0), ▲– total power ($I/I_0 + I'/I'_0$).

of amplifying it. Inversion of population between appropriate energy levels is the main requirement to achieve laser action.

To ensure a more or less equal density of the pumping power along the fiber, the laser resonator must be closed with a totally reflecting output mirror, and the length of the fiber should be chosen in such a way that the reflected power is equal to $I_0/2$ (I_0 – input power), *i.e.*:

$$\frac{I(l_0)}{I_0} = \exp(-\alpha l_0) = 0.5.$$

For $\alpha = 0.004$ cm^{-1} (in our case), we get $l_0 = 174$ cm. In this case, the distribution of the pumping power along the fiber is being kept approximately constant (see Fig. 2). It is thus advisable to measure the α coefficient first.

The threshold for laser action can be written in a simplified form (for a round trip cycle)

$$R_1 R_2 \exp(2\beta l) = 1$$

where R_1, R_2 are reflection coefficients of the mirrors at laser wavelength, and β is the amplification coefficient. Diffraction losses can be neglected in an optical fiber. Coefficients β and α are completely independent of each other, thus, the threshold for laser emission depends also on the amplification length l of the fiber and on the inversion of populations between the transition levels involved. In our case, the threshold for laser emission was found with mirrors $R_1 = 0.98$ and $R_2 = 0.58$, at a launched power density into the fiber of 0.54 MW/cm^2. The double pass gain, $G = \exp(2\beta l) = 1/R_1 R_2 = 1.76$, with $\beta = 0.0016$ cm^{-1}.

It is interesting to note that occasionally, when the incident power launched into the fiber was high enough (> 1 MW/cm^2), and at the highest available quality of the butt-coupling, the output mirror could be replaced by a glass plate, butt-coupled to the fiber terminal, and the laser is still in operation. The glass plate with Fresnel reflection of about 4% is optically better than the fiber terminal, previously cut with a piezoelectrically driven diamond cleaver. Optical flatness and the quality of the butt-coupling (*i.e.*, the Q-factor of the optical cavity) are crucial points in the operation of the fiber laser.

Let us note that β depends linearly on the inversion of populations between the transition levels (see, *e.g.*, [3])

$$\beta = B_{21}\left(N_2 - N_1\right)\frac{h\nu_{21}}{4\pi c}$$

where B_{21} is the well known Einstein coefficient, N_2 and N_1 are populations of the upper and lower laser levels, respectively, ν_{21} is the transition frequency. For $R_1 = 0.98$, $R_2 = 0.04$ and $l \approx 200$ cm, we get:

$$G = \frac{1}{R_1 R_2} = 25.5 \quad \text{and} \quad \beta = 0.0081 \text{ cm}^{-1},$$

which is about 5-times greater than the β-value obtained at lower pumping and smaller Q-factor of the optical cavity.

2.3. Fluorescence at 660 and 850 nm

In a typical infrared-to-visible upconversion laser of ZBLAN:Er^{3+} doped optical fiber, the main fluorescence or laser emission at 544 nm should be much more intense in comparison with the various side emissions, mainly at 660 nm (red) and 850 nm (near IR) – Fig. 4. As we have already found [2], 850 nm emission tends to zero when the pumping wavelength exceeds 807 nm. Using the temperature-tuned laser diode emitting at about 970, we have studied these two side emissions more carefully. Pumping at 970 eliminates practically the 850 nm emission (already discussed in paper [2]), however, the 660 nm one, still exists, due to the $^4F_{9/2} \rightarrow {}^4I_{15/2}$ transition (see Fig. 3).

The red radiation at 660 was also carefully investigated by TAKAHASI *et al.* [4]. Population of the upper $^4F_{9/2}$ level is mainly due to the energy transfer mechanism between the $^4I_{9/2} \rightarrow {}^4I_{13/2}$ and $^4F_{9/2} \rightarrow {}^4I_{11/2}$ transitions. According to the formula derived by Miyakawa and Dexter [5], the probability of multiphonon transitions from a higher j state to the first lower lying level i is

$$W(E_j) = \exp\left[-\alpha\left(E_j - E_i\right)\right].$$

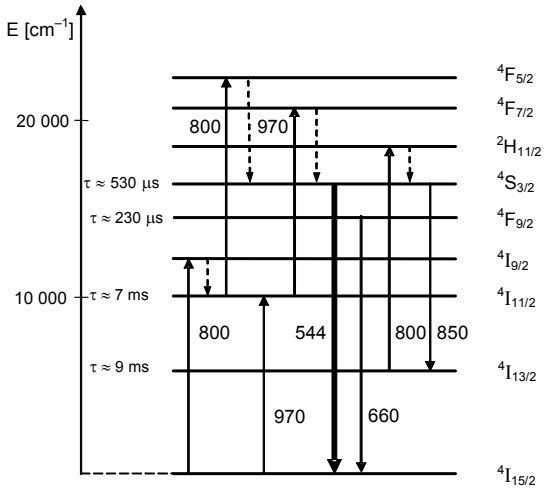

Fig. 3. Simplified energy level diagram of Er^{3+} ion in ZBLAN:Er^{3+} glass. The main transitions are indicated by arrows. The lifetimes τ, in general, depend upon the Er^{3+} concentration. The numbers given in this picture correspond to a typical concentration of about 1000 ppm.

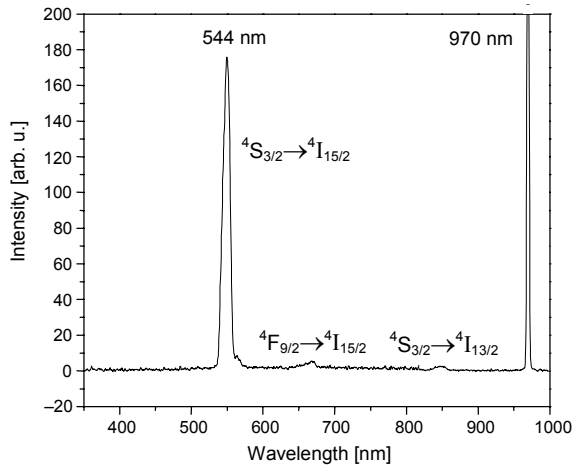

Fig. 4. Undesired side bands at 660 and 850 nm. Their intensities are relatively small in comparison with the main "green" emission at 544 nm.

The "green" emission starts from the $^4S_{3/2}$ level, and the "red" one at 660 nm, from the $^4F_{9/2}$ state. The differences $(E_j - E_i)$ for the two transitions are 3145 and 2814 cm^{-1}, respectively [6]. Thus, the multiphonon quenching of the $^4F_{9/2}$ level is larger than for the $^4S_{3/2}$ one.

Figure 4 illustrates the pumping beam at 970 nm, the main green fluorescence at 544 nm, and the two side emissions at 660 and 850 nm. The emissions at 660 and

850 nm are small enough, and practically do not compete with the desired green emission at 544 nm.

Acknowledgement – Thanks are due to the Foundation for Polish Science (Fundacja na Rzecz Nauki Polskiej) for its financial support under SUBIN Grant No. 25/2004.

References

[1] KACZMAREK F., *Laser diode pumping of an upconversion laser*, Optica Applicata **31**(2), 2001, pp. 373–6.

[2] KACZMAREK F., KAROLCZAK J., *Infrared-to-visible upconversion in erbium fluoride (ZBLAN:Er^{3+}) optical fiber: competition between the parasitic 850-nm fluorescence and the green laser emission at 544 mn*, Opto-Electronics Review **12**(2), 2004, pp. 247–8.

[3] O'SHEA D.C., CALLEN W.R., RHODES W.T., *Introduction to Lasers and Their Applications*, Addison-Wesley 1977.

[4] TAKAHASHI M., SHOJIYA M., KANNO R., KAWAMOTO Y., KADONO K., OHTSUKI T., PEYGHAMBARIAN N., *Nonradiative decay processes and mechanisms of frequency upconversion of Er^{3+} in ZrF_4-BaF_2-LaF_3 glass*, Journal of Applied Physics **81**(7), 1997, pp. 2940–5.

[5] MIYAKAWA T., DEXTER D.L., *Photon sidebands, multiphonon relaxation of excited states, and phonon-assisted energy transfer between ions in solids*, Physical Review B: Solid State **1**(7), 1970, pp. 2961–9.

[6] SHINN M.D., SIBLEY W.A., DREXHAGE M.G., BROWN R.N., *Optical transitions of Er^{3+} ions in fluorozirconate glass*, Physical Review B: Condensed Matter **27**(11), 1983, pp. 6635–48.

Received July 19, 2005